Lab on a Chip

PAPER

View Article Online
View Journal | View Issue

Cite this: *Lab Chip*, 2015, **15**, 3335

Scalable single-step microfluidic production of single-core double emulsions with ultra-thin shells†

L. R. Arriaga,‡ E. Amstad‡§ and D. A. Weitz*

Received 8th June 2015,
Accepted 2nd July 2015

DOI: 10.1039/c5lc00631g

www.rsc.org/loc

We report a versatile and robust device for the continuous production of double emulsion drops with very thin shell thicknesses, of about 5% of the radius: for emulsions 50 μm in radius the shells can be as thin as a few micrometers. Importantly, the viscosity of the oil shell can be varied from that of water up to 70 times that of water without compromising device operation. Furthermore, this device can be easily scaled-up as it is made through soft lithography; this may enable the production of industrial quantities of double emulsion drops with ultra-thin shells, which may serve as templates to form capsules with homogeneous shell thicknesses, useful beyond scientific applications.

Introduction

Single-core double emulsions are liquid drops, each one surrounded by a shell that is composed of a second, immiscible liquid. These are used as templates to form many types of capsules through solidification of the emulsion shell.[1] These capsules serve as vehicles for the delivery of different ingredients including, for example, food additives,[2–4] pharmaceuticals,[5,6] and cosmetics actives.[7,8] However, these applications depend critically on the permeability and mechanical stability of the capsule shell, parameters that strongly depend on the composition and thickness of the shells of the double emulsion drops used as templates; thus, these parameters must be carefully controlled during capsule fabrication. The excellent control over the fluid flow afforded by microfluidics enables the production of highly monodisperse double emulsion drops whose composition is well defined.[9,10] However, most often, the fluids that make up the double emulsion drops have different densities and thus, the centers of the inner and outer drops of the double emulsions are off-set;[11] this results in capsules with inhomogeneous shell thicknesses.[12] Capsules with homogeneous shell thicknesses can be made from double emulsion drops with very thin shells as the offset of the centers of the drops is then minimal; this is mainly due to their higher lubrication resistance.[13] Such double emulsion drops can be produced in a single emulsification step using microfluidic glass capillary devices.[11] Unfortunately, this device is difficult to scale up as every device is aligned manually and is thus unique; even if differences in each device are small, flow rates typically must be adjusted for each device individually. By contrast, devices produced through soft lithography are all much more nearly identical as they are made from masters; this makes their parallelization easier. Indeed, up to 15 microfluidic double emulsion devices have been parallelized.[14] However, these devices produce double emulsions in two steps resulting in thick shells. Double emulsions with thin shells have been produced using PDMS.[15] However, these devices also utilize sequential emulsification and rely on a delicate interplay between surface coating and inertial forces, which makes their operation difficult. The design of a scalable PDMS-based microfluidic device that produces double emulsions with thin shells in a continuous fashion remains an unmet, yet important challenge.

In this paper, we report a microfluidic device, made through soft lithography, which enables the continuous production of double emulsions with very thin shell thicknesses, of about 5% of the radius, through a single-step emulsification process. The size and shell thickness of the double emulsions can easily be tuned by varying either the flow rates of the fluids or the height of the tapered region of the injection channel. Moreover, the shell thickness can be further decreased by squeezing double emulsion drops through constrictions. We demonstrate the versatility of the device by producing double emulsion drops from oils with viscosities ranging from that of water up to 70 times that of water. Furthermore, we demonstrate the feasibility of scale-up of this

School of Engineering and Applied Sciences and Department of Physics, Harvard University, Cambridge, MA, 02138, USA. E-mail: weitz@seas.harvard.edu

† Electronic supplementary information (ESI) available: High-speed camera movies showing generation of double emulsions with thin shells (S1), removal of oil using a constriction (S2 and S3) and simultaneous operation of three parallelized devices (S4). See DOI: 10.1039/c5lc00631g

‡ These authors contributed equally to this work.

§ Present address: School of Engineering, Ecole Polytechnique Federale de Lausanne, CH-1015, Switzerland.

process by parallelizing three individual drop makers on a single chip, using a common feed for each fluid. Our work thus constitutes a versatile, robust and scalable approach for the continuous fabrication of double emulsion drops with ultra-thin shells.

Results and discussion

Our microfluidic device is made of polydimethylsiloxane (PDMS) and fabricated using soft lithography.[16,17] It consists of three inlets to inject the inner, middle and outer phases and an outlet to collect double emulsion drops as shown by the arrows in Fig. 1. The inner phase, an aqueous solution of 10 wt% poly(ethylene glycol) (PEG, 6 kDa) is injected into the first inlet and thus flows through the main channel, which is initially 30 μm tall and 50 μm wide. The middle oil phase, a solution of 20 wt% Krytox-PEG-Krytox dissolved in a perfluorinated oil (HFE 7500) is injected into the second inlet and flows through a pair of channels that intersect the main channel at an angle of 45°, as shown in Fig. 1 on the left. At this junction, the width of the main channel increases to 100 μm. The main channel width is then tapered from 100 to 20 μm and its height is varied from 30 to 10 μm; this configuration mimics the tip of the injection capillary of a co-flow glass capillary device.[11] We treat the main channel upstream this tip with a solution of 1 vol% perfluorinated trichlorosilane dissolved in HFE 7500 to render its surface fluorophilic, thus preventing wetting of the innermost water phase on the main channel wall. We inject the inner and middle phases at a flow rate of 1 and 0.4 mL h^{-1}, respectively; under these conditions the innermost aqueous phase forms a stable jet, surrounded by a thin layer of perfluorinated oil, within the main channel. We then inject the outer phase, an aqueous solution of 10 wt% poly(vinyl alcohol) (PVA, 13–23 kDa) into the third inlet at a flow rate of 3 mL h^{-1}; this phase flows through a pair of channels that intersect the main channel at the tip at an angle of 45°. At this junction the height of the main channel increases abruptly from 10 to 50 μm. We treat the main channel downstream the tip with a cationic polyelectrolyte solution that contains 1 vol% of poly(diallyldimethylammonium chloride) (400–500 kDa) and 2 M of NaCl to make the channel walls hydrophilic,[18] thus preventing wetting of the middle oil phase on its walls. This protocol forces the stable water jet to break up into monodisperse water-in-oil-in-water (W/O/W) double emulsion drops with ultra-thin shells as shown in Fig. 1 and Movie S1 of the ESI.† To avoid osmotic stresses we collect the resultant double emulsions in a sucrose solution having the same osmolarity (100 mOsM) as their innermost water cores.

We operate the device downstream the tip in the dripping regime to ensure that the resultant double emulsion drops are monodisperse in size, as shown in the optical microscope images of Fig. 2(a–d), with typical coefficients of variation

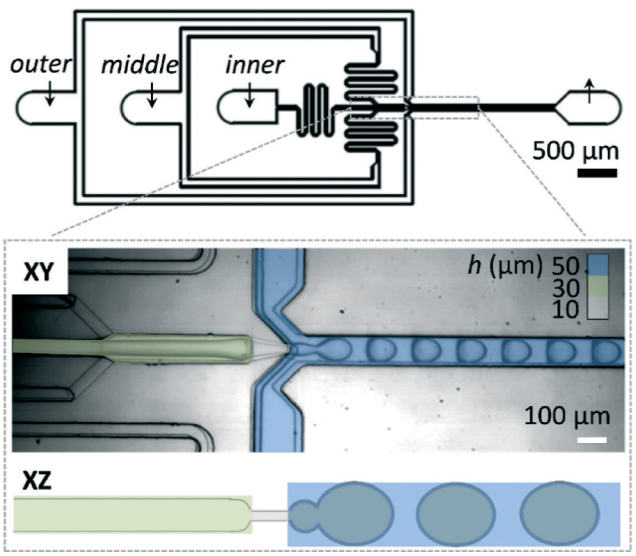

Fig. 1 Microfluidic production of double emulsion drops with thin shells at typical flow rates of the inner, middle and outer phases of 1, 0.4 and 3 mL h^{-1}, respectively, using a PDMS device that contains three different heights as shown by the different colors and by the schematic illustration of the side view of the device.

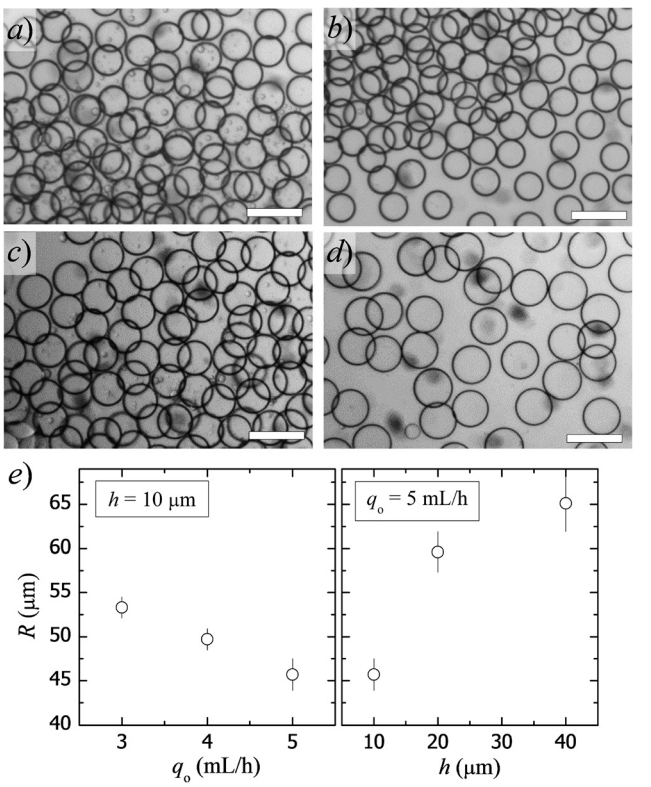

Fig. 2 Optical microscope images of double emulsion drops produced with a device with a tip that is 10 μm high, at typical flow rates of the inner, middle and outer phases of (a) 1, 0.4 and 3 mL h^{-1} and (b) 1, 0.4 and 4 mL h^{-1}, respectively. Optical microscope images of double emulsion drops produced at typical flow rates of the inner, middle and outer phases of 1, 0.4 and 5 mL h^{-1}, respectively, with a device with a tip that is (c) 20 μm and (d) 40 μm. Scale bars are 200 μm. (e) Variation of the radius, R, of the double emulsions as a function of the flow rate of the outer phase, q_o and as a function of the height of the tapered region, h, of the PDMS device.

ranging from 2 to 5%. In this regime, much like for single emulsion drops, breakup of double emulsions is governed by the competition between the capillary force that pins the drop to the tip and the shear force exerted by the outer phase that pulls the drop off of the tip. The capillary force is proportional to the interfacial tension between the middle oil and the outer water phases, $\gamma_{m/o}$, and to the tip dimensions. In addition, as the middle oil phase breaks up before the inner water phase does, the shear force is proportional to the viscosity of the outer phase, η_o, and to the difference in the average velocity between the outer and middle phases.[19] Therefore, by finely tuning any of these parameters, we can control the size of the resultant double emulsions. For example, if we increase the flow rate of the outer phase, q_o, the radius of the double emulsions, R, decreases as shown in the leftmost panel of Fig. 2(e). In the same fashion, if we increase the tip dimensions, in particular the height of the tip, h, the radius of the double emulsions increases as shown in the rightmost panel of Fig. 2(e).

The thickness, t, of the double emulsion drops produced with this device is too small to be measured directly with our optical microscope. In addition, these double emulsions are very stable and thus difficult to rupture. Therefore, to measure their shell thickness, we compress them in the vertical direction by confining them in between two microscope cover glasses; this makes them expand in the horizontal direction as illustrated schematically in Fig. 3(a) and exemplified by Fig. 3(b). The resultant shape of the compressed emulsions is a spheroid that conserves the volume of the initially spherical double emulsions. This condition of volume conservation allows us to determine the thickness of the double emulsions as,

$$t = R[1 - (r_c/R_c)^{2/3}],$$

where R is the actual radius of the outer drop of the double emulsions, and R_c and r_c are the radius of the outer and inner drops of the double emulsions in the compressed situation, respectively. We confirm that the equatorial plane of our emulsion drops remain circular under compression; this allows us to measure R_c and r_c as shown in Fig. 3(b). This procedure constitutes a non-destructive method for estimating small shell thicknesses.

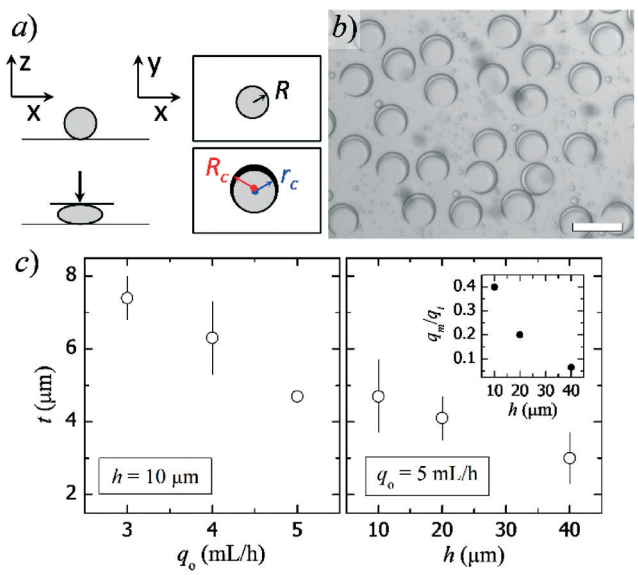

Fig. 3 (a) Schematic illustration of the changes in the vertical and horizontal dimensions of the double emulsions upon compression. The centers of the inner and outer drops are off-set under compression. (b) Optical microscope images of double emulsion drops produced with a device with a tip that is 10 μm high, at typical flow rates of the inner, middle and outer phases of 1, 0.4 and 4 mL h^{-1}, respectively, upon compression. Scale bar is 200 μm. (c) Variation of the thickness, t, of the double emulsions as a function of the flow rate of the outer phase, q_o and as a function of the height of the tapered region, h, of the PDMS device. Inset: the volumetric ratio of the middle to the inner phase is decreased upon increasing h.

The thickness of the double emulsions is determined by the difference between the radius of the outer drop, R, and that of the inner drop, r. Whereas R decreases upon increasing q_o, r is fixed by the mass balance between the inner and middle phases and thus, does not depend on q_o.[15] Therefore, we expect the thickness of the double emulsions to decrease with q_o. In good agreement with this expectation, the thickness of the double emulsions decreases from 7.4 to 4.7 μm if q_o is increased from 3 to 5 mL h^{-1}, as shown in the leftmost panel of Fig. 3(c). In the same fashion, if the height of the tip is increased, one expects the thickness of the double emulsions to increase. However, increasing h allows us to operate the device at a lower volumetric ratio of the middle to the inner phase as shown in the inset of Fig. 3(c); this results in a reduction of the shell thickness of the double emulsions from 4.7 μm to 3.0 μm by changing from a tip that is 10 μm high to one that is 40 μm high, as shown in the rightmost panel of Fig. 3(c).

A further decrease in the thickness of the shell of the double emulsions can be achieved by exploiting the delicate interplay between the deformation of the droplets under flow and their contact with the channel walls. To achieve this, we incorporate a constriction of width 20 μm and length 200 μm in the collection channel of our double emulsion drop maker as shown in Fig. 4(a) and Movies S2 and S3 of the ESI.† Within this constriction, the droplets accelerate. Since the density of the water cores of the double emulsions is lower than that of their oil shells, they travel faster; this forces the oil towards the tailing end of the drop. This accumulation of oil breaks up into droplets upon contact of the channel walls; the single emulsion droplets that result from this breakup are enclosed by the circles in Fig. 4(a). The incorporation of a second constriction, located 200 μm apart from the first one, further reduces the shell thickness, as shown by the solid symbols in Fig. 4(b). However, incorporation of more than three constrictions compromises the operation of the device as it further increases the hydrodynamic resistance of the channel. Instead, we collect these double emulsions and re-inject them into microfluidic channels that comprise up to three constrictions to further reduce their shell thickness, as

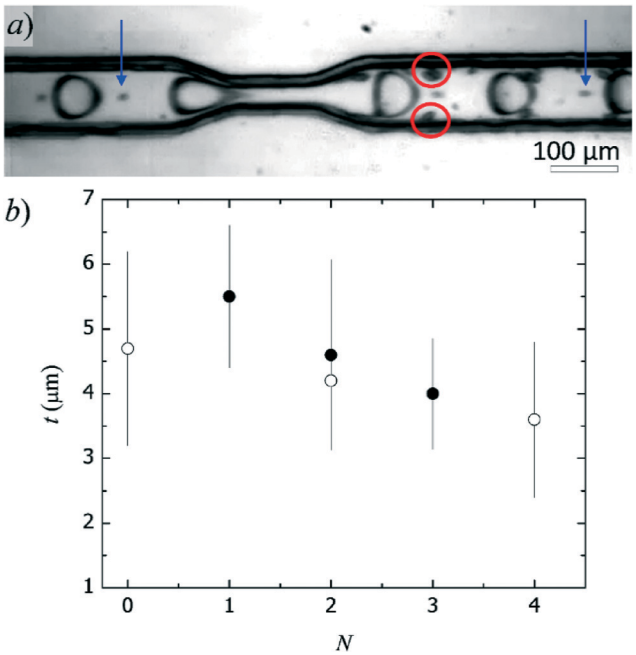

Fig. 4 (a) Optical microscope image showing removal of oil from the shell of double emulsions through the use of constrictions. Removed oil droplets are shown by red circles; satellite droplets resulting from the production are indicated by blue arrows. (b) Variation of the shell thickness as a function of the number of constrictions. Data represented by solid symbols are obtained if constrictions are incorporated in the double emulsion drop maker device; data represented by hollow symbols are obtained after re-injection of double emulsions into a straight channel with a certain number of constrictions.

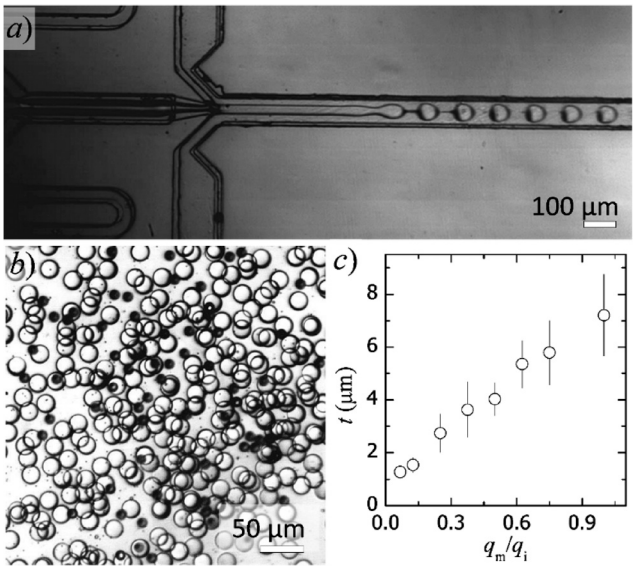

Fig. 5 (a) Microfluidic production of double emulsion drops with thin shells in the jetting regime for a highly viscous middle phase that consists of ETPTA. (b) Optical microscope image of the resultant double emulsion droplets. Black droplets are single emulsion drops that result from rupture of double emulsion drops. (c) Thickness of the double emulsions as a function of the ratio of flow rates of the middle oil to the inner water phase.

shown by the open symbols in Fig. 4(b). To achieve this decrease in shell thickness without breaking our double emulsion drops, we use a maximum flow rate of 5 mL h^{-1} in our re-injection experiments.

One difficulty in producing these emulsions occurs when using highly viscous middle phases. However, this is important because the precursors commonly required to form many different types of capsules through polymerization are highly viscous. Therefore, we demonstrate the capability of the device to produce double emulsion droplets employing, as a middle phase, ethoxylated trimethylolpropane triacrylate (ETPTA), a monomer with a viscosity 70 times that of water that can be cross-linked using ultraviolet light to form solid polymer capsules. To ensure wetting of ETPTA on the wall of the injection channel, we make it hydrophobic using a solution of 1 vol% dodecyltrichlorosilane dissolved in heptadecane. In this case, due to the high viscosity of ETPTA, the device can only be operated in the jetting mode as shown in Fig. 5(a); nevertheless, the resultant double emulsions are still monodisperse as shown in Fig. 5(b). If the monomer in the shell is not polymerized immediately the double emulsions rupture, thereby yielding single emulsion drops from the shells. We measure the diameter of these single emulsion drops to determine the initial thickness of the double emulsions as a function of the ratio of the middle to the inner phase flow rates as shown in Fig. 5(c). Remarkably, the shell of these emulsions can be made as thin as 1 μm, but they must be stabilized through polymerization.

To demonstrate the scalability of this device, we parallelize three individual drop makers as this is the minimum number of devices that ensures the lack of hydrodynamic coupling of the drop formation. We use a single distribution channel for each of the fluids. The distribution channels are made from PDMS and have a typical width of 500 μm and height of 200 μm. We bond these distribution channels onto the PDMS chip to operate the three devices simultaneously, while using a single pump for each channel, as shown in Movie S4 of the ESI.† The production rate of these parallelized devices is of 4.5 mL of double emulsion drops per hour. Importantly, this method is not restricted to the parallelization of only three devices but allows numbering up many more; this further enhances the potential of this device to produce large quantities of size monodisperse double emulsions with very thin shells.

Experimental

Device fabrication

We fabricate our devices from masters made with a negative photoresist, SU-8 (Microchem), though soft lithography.[16,17] However, because our device includes steps in height both upwards and downwards, we pattern both the top and bottom halves of the device using two different masters.[20] The first half includes three layers. The thickness of the first layer of the first half is varied from 10 to 40 μm; this makes the

height of the device tip, h, vary from 10 to 40 μm. The thickness of the second and third layers are both 10 μm. The second half includes only the second and third layers, which are both 10 μm. We generate the devices from Sylgard 184 polydimethylsiloxane (PDMS, Dow Corning), which we mix at 1 : 10 mass ratio, pour it over the mold, degass it for 20 min under vacuum, and cure it at 65 °C for 12 h. The replica is then removed from the mold and the holes for the inlets and outlet are made in one of the halves, using a biopsy punch with an inner diameter of 1 mm. We align the two halves[21] and plasma bond them together;[22] this results in a device that is (20 + h) μm high upstream the tip and (40 + h) μm high downstream the tip. For the parallelized devices, we plasma bond the distribution channels on top of the device after they are assembled.

Device surface functionalization

Surface functionalization is critical for device functioning. We treat the main channel downstream the tip with a cationic polyelectrolyte that consists of an aqueous solution of 1 vol% poly(diallyldimethylammonium chloride) and 2 M NaCl. We gently inject this solution into the outermost channel, ensuring that it does not flow into the device tip. To make perfluorinated double emulsions, we make the main channel upstream the tip fluorophilic by connecting the first inlet of the device to a syringe that contains a solution of 1 vol% perfluorinated trichlorosilane in HFE. By contrast, to make double emulsions with hydrocarbon-based shells, we treat the main channel upstream the tip with a solution of 1 vol% dodecyltrichlorosilane in heptadecane. We inject this solutions through the first inlet while the main channel downstream the tip is still filled with the polyelectrolyte solution to prevent flow of the silane-based solution into the main channel downstream the tip. After 5–10 min, we remove the solutions from the device. To do this, we disconnect all the syringes and remove the remaining polyelectrolyte solution by injecting pure water through the outermost channel. We subsequently dry the device by pushing air through all the channels.

Imaging

Images and movies are acquired using a 5× objective on an inverted microscope (Leica) equipped with a high speed camera (Phantom V9). Sizes and thicknesses of the emulsion droplets are measured using ImageJ.

Conclusions

Our PDMS-based double emulsion drop maker produces monodisperse double emulsions, with shells as thin as 1 μm, while operating in a continuous fashion. A single device is approximately 15 mm long, 5 mm wide and 140 μm high; therefore, it occupies a volume of approximately 10 μL. As the device is produced using soft lithography, it could be easily parallelized. Indeed, 10^5 of these devices could be packed into 1 L, for example arranging them in several columns and connecting them with holes within each column and with distribution channels on the top layer; this would result in the production of 150 L of drops per hour from a volume of 1 L, as every single device could be operated at approximately 1.5 mL h^{-1}. Therefore, this device has the potential to make large quantities of monodisperse emulsions with thin shells; these may serve as templates to make capsules with very homogeneous shell thicknesses, useful beyond scientific applications. Furthermore, this device, with an appropriate surface treatment, might be used to produce single-core O/W/O or gas/O/W double emulsion droplets.[23]

Acknowledgements

This work was supported by the National Science Foundation (DMR-1310266), the Harvard Materials Research Science and Engineering Center (DMR-1420570) and a Marie Curie International Outgoing Fellowship within the EU Seventh Framework Programme for Research and Technological Development (2007–2013). Part of this work was performed at the Center for Nanoscale Systems (CNS), a member of the National Nanotechnology Infrastructure Network (NNIN), which is supported by the National Science Foundation under NSF award no. ECS-0335765. CNS is part of Harvard University.

Notes and references

1 S. S. Datta, A. Abbaspourrad, E. Amstad, J. Fan, S.-H. Kim, M. Romanowsky, H. C. Shum, B. Sun, A. S. Utada, M. Windbergs, S. Zhou and D. A. Weitz, *Adv. Mater.*, 2014, **26**, 2205–2218.
2 A. Downham and P. Collins, *Int. J. Food Sci. Technol.*, 2000, **35**, 5–22.
3 H. Hatcher, R. Planalp, J. Cho, F. M. Torti and S. V. Torti, *Cell. Mol. Life Sci.*, 2008, **65**, 1631–1652.
4 L. Chen, G. E. Remondetto and M. Subirade, *Trends Food Sci. Technol.*, 2006, **17**, 272–283.
5 D. C. Bibby, N. M. Davies and I. G. Tucker, *Int. J. Pharm.*, 2000, **197**, 1–11.
6 C. E. Mora-Huertas, H. Fessi and A. Elaissari, *Int. J. Pharm.*, 2010, **385**, 113–142.
7 K. Miyazawa, I. Yajima, I. Kaneda and T. Yanaki, *J. Cosmet. Sci.*, 2000, **51**, 239–252.
8 M. Jacquemond, N. Jeckelmann, L. Ouali and O. P. Haefliger, *J. Appl. Polym. Sci.*, 2009, **114**, 3074–3080.
9 A. S. Utada, E. Lorenceau, D. R. Link, P. D. Kaplan, H. A. Stone and D. A. Weitz, *Science*, 2005, **308**, 537–541.
10 J.-H. Xu, X.-H. Ge, R. Chen and G.-S. Luo, *RSC Adv.*, 2014, **4**, 1900–1906.
11 X.-H. Ge, J.-P. Huang, J.-H. Xu and G.-S. Luo, *Lab Chip*, 2014, **14**, 4451–4454.
12 S. S. Datta, S.-H. Kim, J. Paulose, A. Abbaspourrad, D. R. Nelson and D. A. Weitz, *Phys. Rev. Lett.*, 2012, **109**, 134302.
13 S.-H. Kim, J. W. Kim, J.-C. Cho and D. A. Weitz, *Lab Chip*, 2011, **11**, 3162–3166.

14 M. B. Romanowsky, A. R. Abate, A. Rotem, C. Holtze and D. A. Weitz, *Lab Chip*, 2012, **12**, 802–807.
15 D. Saeki, S. Sugiura, T. Kanamori, S. Sato and S. Ichikawa, *Lab Chip*, 2010, **10**, 357–362.
16 Y. N. Xia and G. M. Whitesides, *Angew. Chem., Int. Ed.*, 1998, **37**, 551–575.
17 J. C. McDonald, D. C. Duffy, J. R. Anderson, D. T. Chiu, H. Wu, O. J. A. Schueller and G. M. Whitesides, *Electrophoresis*, 2000, **21**, 27–40.
18 W.-A. C. Bauer, M. Fischlechner, C. Abell and W. T. S. Huck, *Lab Chip*, 2010, **10**, 1814–1819.
19 R. M. Erb, D. Obrist, P. W. Chen, J. Studer and A. R. Studart, *Soft Matter*, 2011, **7**, 8757–8761.
20 A. Rotem, A. R. Abate, A. S. Utada, V. V. Steijn and D. A. Weitz, *Lab Chip*, 2012, **12**, 4263–4268.
21 J. R. Anderson, D. T. Chiu, R. J. Jackman, O. Cherniavskaya, J. C. McDonald, H. Wu, S. H. Whitesides and G. M. Whitesides, *Anal. Chem.*, 2000, **72**, 3158–3164.
22 M. K. Chaudhury and G. M. Whitesides, *Langmuir*, 1991, **7**, 1013–1025.
23 R. Chen, P.-F. Dong, J.-H. Xu, Y.-D. Wang and G.-S. Luo, *Lab Chip*, 2012, **12**, 3858–3860.

